Available online at www.sciencedirect.com
SCIENCE DIRECT®
Journal of Solid State Chemistry 174 (2003) 424–430
JOURNAL OF SOLID STATE CHEMISTRY
http://elsevier.com/locate/jssc

Raman spectroscopic study of magnetite ($FeFe_2O_4$): a new assignment for the vibrational spectrum

Olga N. Shebanova* and Peter Lazor

Department of Earth Science, Uppsala University, SE-752 36 Uppsala, Sweden

Received 2 February 2003; received in revised form 9 May 2003; accepted 17 May 2003

Abstract

A detailed Raman study on natural magnetite has been carried out. Raman spectra show four out of the five predicted Raman bands located at 668, 538, 306, and 193 rcm^{-1}. The location of the fifth, unobserved phonon mode, is inferred from spectra of other ferrites at 450–490 rcm^{-1}. Polarized experiments on an oriented single crystal provide a new interpretation of the Raman spectrum with the following assignment for symmetries of the observed modes: A_{1g} for 668 rcm^{-1}, E_g for 306 rcm^{-1}, and T_{2g} for 538, 193, and 450–490 rcm^{-1}. The results are compared with those of the earlier Raman studies and possible explanations for the discrepancies are suggested. Some of the inconsistencies can be resolved by considering the effect of oxidation of magnetite during the Raman experiments.

Keywords: Magnetite; Raman spectroscopy; Spinel; Polarization

1. Introduction

Due to its geological and technological importance, and interesting physical properties, the iron oxide magnetite Fe_3O_4 has been subjected to a large number of studies employing different kinds of experimental techniques and theoretical approaches [1–6]. Yet, despite the intense effort and significant advances, understanding some of its fundamental properties still remains an elusive goal. It is an intimate interplay of structural, electronic, and magnetic properties that makes the studies on this compound so difficult. Effects of order–disorder of cations between octahedral and tetrahedral sites, nonstoichiometry, presence of impurities and defects, oxidation, sample history and origin (e.g., natural vs. synthetic crystals), have to be disentangled in order to reveal the genuine intrinsic properties. Vibrational spectroscopy, both infrared and Raman, proved to be a powerful tool for a direct probing of lattice dynamics of this compound, particularly in the temperature dependent studies of optical phonons across the Verwey transition.

Raman measurements on magnetite have been carried out in several studies. Some of these were devoted to magnetite itself [1,4,7–11] while in others magnetite was considered as a secondary product of reactions [12–15]. A symmetry analysis and an assignment of magnetite phonon modes based on the spinel structure were carried by Verble [7], Degiorgi et al. [9], Hart et al. [8], Graves et al. [16] and Gasparov et al. [1]. The results of these studies vary significantly either in the number of the observed Raman modes, or their positions and assignments. In this paper we present results obtained from a careful analysis of our extensive polarized Raman measurements, a critical evaluation of previously published spectroscopic studies on magnetite, and from the systematics of Raman spectra of ferrites.

2. Experimental details

2.1. Sample characterization

The sample of natural magnetite comes from the metamorphosed iron formation in Grängesberg, Sweden. The chemical composition is presented in Table 1 [17]. The unit-cell constant determined by

*Corresponding author. Fax: +46-18-471-2591.
E-mail address: olga.shebanova@geo.uu.se (O.N. Shebanova).

0022-4596/03/$ - see front matter © 2003 Elsevier Inc. All rights reserved.
doi:10.1016/S0022-4596(03)00294-9

Table 1
The content of trace elements in the studied sample of natural magnetite (ppm)

Zn	59
Pb	9
Cu	11
Co	41
Ni	92
Mn	365
Ti	425>
V	1920
Cr	17
Mo	4
Cd	1.0

X-ray powder diffraction has the value $a = 8.3945(11)$ Å, which is in a good agreement with published data for natural Fe_3O_4 $a = 8.3941(7)$ Å [18]. The polarized Raman spectra were taken from the polished (100) face of the single crystal of magnetite.

2.2. Experimental methods

The light-scattering experiments were conducted using a single stage imaging spectrograph (Oriel) equipped with a thermoelectrically cooled (−60°C) CCD detector (Andor). The Raman spectra were excited by the 514.5 nm line of an argon ion laser (Coherent, Innova) and collected in a backscattering geometry with spectral resolution 6 cm^{-1}. Two holographic supernotch filters (Kaiser) were used to suppress the Raleigh line. The laser beam was focused on the sample by a $\times 20$ lens to a spot size of ca. 5–10 μm. The reported Raman frequencies have uncertainties $\pm 1.5\,cm^{-1}$. The laser power reaching the sample surface was ca. 7 mW. The typical acquisition time was 60 s. Some polarized spectra were collected also with a newly acquired holographic imaging spectrograph (HoloSpec, Kaiser) in an identical set-up.

3. Results and discussion

Above the Verwey transition temperature ($T_v = 121$ K), the iron oxide magnetite $Fe^{3+}(Fe^{2+}Fe^{3+})O_4$ crystallizes in the cubic space group $Fd3m$ (O_h^7), $Z = 8$. It represents the classical example of an inverse spinel ferrite AB_2O_4. Oxygen atoms, having general positions 32*e*, form approximately a close-packed face centered cubic arrangement. The iron atoms occupy two crystallographically distinct sites being tetrahedrally $A(8a)$ and octahedrally $B(16d)$ coordinated by oxygen anions. The inverse nature of this spinel implies that the *A*-sites are occupied by Fe^{3+} ions, while an equal number of Fe^{2+} and Fe^{3+} cations share the *B*-site. The dynamic electronic disorder resulting from the rapid electron exchange (hopping) between Fe^{2+} and Fe^{3+} cations on the *B*-site is responsible for the high electrical conductivity of magnetite above the Verwey transition. However, recent studies [5,6] criticize this charge-density-fluctuation model and assert that the electrons at the *B*-sites are of itinerant nature (delocalized), thus abandoning the traditional view on magnetite as an example of the mixed-valence compound.

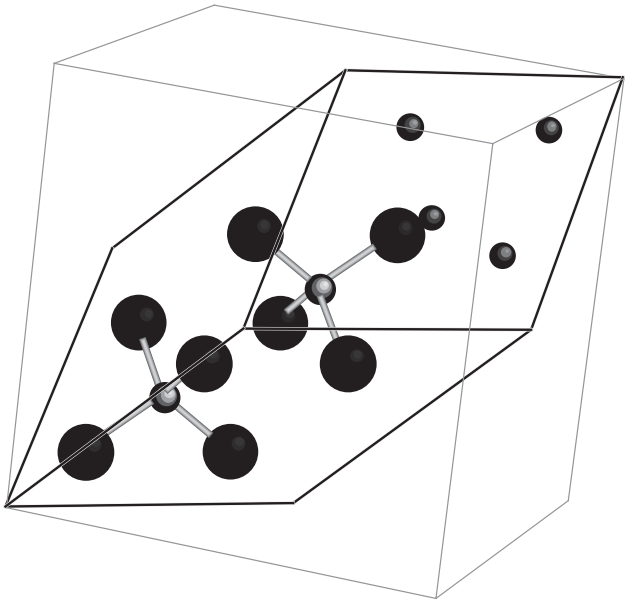

Fig. 1. Primitive unite cell of magnetite ($Z = 2$). Large spheres represent oxygen atoms with site symmetry $3m$ (C_{3v}); two tetrahedrally coordinated linked spheres depict atoms of ferric iron $\bar{4}3m$ (T_d); four small spheres show atoms of iron with non-integer valence state +2.5 occupying octahedral positions $\bar{3}m$ (D_{3d}).

The site symmetries of Wyckoff positions in the primitive unit cell (Fig. 1) containing 14 atoms are $\bar{4}3m$ (T_d), $\bar{3}m$ (D_{3d}), and $3m$(C_{3v}). Due to the delocalized nature of electrons, the *B*-site retains the local D_{3d} symmetry, which otherwise becomes lowered in an inverse spinel. The theoretical analysis based on the factor-group approach predicts five Raman-active bands A_{1g}, E_g and three T_{2g}, and four infrared-active bands T_{1u} [19]. The presence of an inversion center in the centrosymmetrical space group $Fd3m$ implies mutual exclusion of Raman and infrared activities for the same vibrational modes. Only the sites T_d and C_{3v} occupied by Fe^{3+} and O^{2-} ions, respectively, contribute to the Raman activity. This fact is of practical use when comparing spectra of cation-substituted spinels in their systematic studies and helps us to locate the approximate position of one unobserved Raman band.

Grimes [20,21] proposed that the true space group of cubic spinels, including ferrites and particularly magnetite, is less symmetrical than $Fd3m$ due to a small displacement of an octahedral cation along the [111] direction. Using the results of X-ray diffraction [21]

along with other experimental evidence [20] the non-centrosymmetric structure $F\bar{4}3m$ (T_d) was assumed. The proposed distortion, however, is very small and has not yet been confirmed by later studies. From purely group-theoretical point of view, the proposed structure exhibits 14 Raman active modes ($3A_1 + 3E + 8T_2$) and could, in principle, be detected by the occurrence of splitting of the E_g and T_{2g} modes.

At ambient conditions, the nonpolarized spectrum of magnetite shows four out of the five theoretically predicted phonon bands at 668, 538, 306, and 193 rcm^{-1} (Fig. 2). The mode at 193 rcm^{-1} is weak and is only reported in Ref. [1] (Table 2). In fact, a weak peak at 193 cm^{-1} is also visible but not reported in a spectrum of magnetite taken by de Faria (Fig. 3 in Ref. [10]). In our study, the existence of this phonon is confirmed by its presence on the anti-Stoke side of the spectrum (Fig. 2).

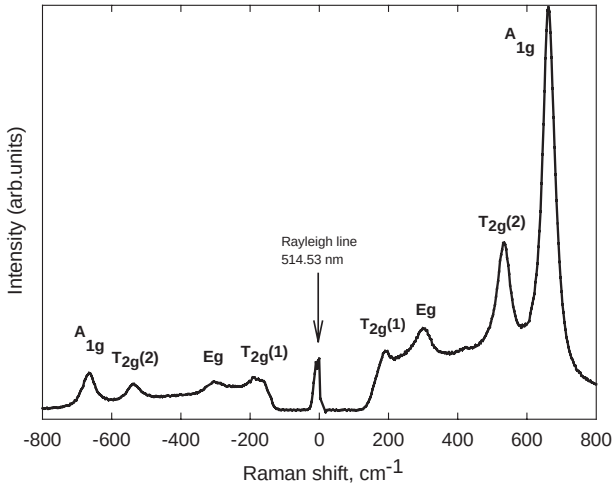

Fig. 2. Raman spectrum of magnetite with the symmetry assignment.

Table 2
Overview of Raman mode frequencies reported in different studies

Reference	Raman shift (rcm^{-1})						
Verble et al. [7][a]	680	560		420	320	300	
Boucherit et al. [15]	670	550					
Hart et al. [8]	676	550	472	420	320	298	
Dunnwald and Otto [14] 1322	676	550	470	418	319	298	
Ohtsuka et al. [12]	665	540					
Thierry et al. [13]	670	550					
de Faria et al. [10]	662.7	533.6			301.6		
Gasparov et al. [1]	670	540			308		193
Degiorgi et al. [9][b]	672	542	462	410	318		160
Graves et al. [16]	706	570	490		336		226
Li and Huan [11]	665	540			311		
Bersani et al. [25]	666	541			311		
Gupta et al. [4]	669	540		410	300		
Present study	668	538			306		193

[a] At 77 K
[b] At 130 K.

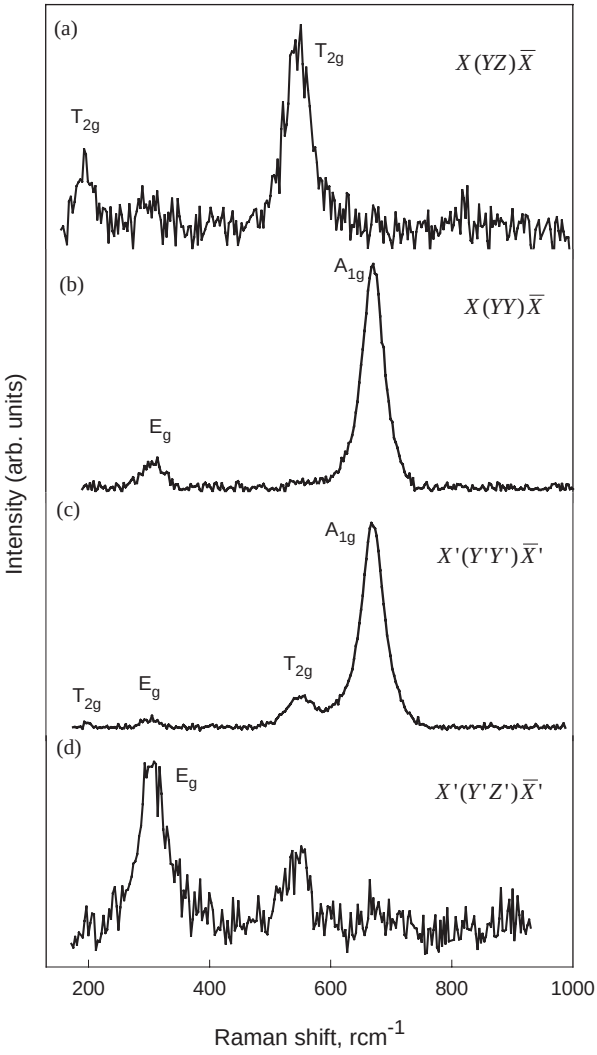

Fig. 3. Polarization Raman spectra of magnetite at ambient temperature: (a) spectrum taken from crystal oriented in the crystallographic frame of reference; incident and scattered laser beams have perpendicular polarization—$X(YZ)\bar{X}$; (b) the same orientation of the crystal; incoming and scattered beams polarized parallel—$X(YY)\bar{X}$; (c) crystal rotated by 45° around x-axis, polarizations parallel—$X'(Y'Y')\bar{X}'$ geometry; (d) the crystal oriented as in (c); incident and scattered beams are perpendicular—$X'(Y'Z')\bar{X}'$.

Another weak band observed at 410 rcm^{-1} is not always documented in a Raman pattern. Its nature will be discussed below.

The results of this and previously published Raman studies on magnetite are presented in Table 2. Inspection of data shows that while there is an acceptable consistency for the strongest modes at ~666, ~538, and ~306 rcm^{-1}, the agreement for the remaining modes is less satisfactory. The data from Verble [7] are taken below the Verwey transition where magnetite is transformed to an orthorhombic phase. The presence of a peak at 298 rcm^{-1} in studies by Dunnwald and Otto [14], and Hart et al. [8] suggests a beginning of oxidation, especially when associated with lines around

Table 3
Comparison of frequencies of Raman modes between magnetite and some inverse ferrites

Ferrites	Symmetry and Raman shift (rcm^{-1})					Ref.
	T_{2g}	E_g	T_{2g}	T_{2g}	A_{1g}	
$FeFe_2O_4$	193	306		538	668	This work
$FeFe_2O_4$[a]	226	336	490	570[b]	706	[16]
$NiFe_2O_4$		339	490	579[b]	700	[16]
$MnFe_2O_4$		331	496	543[b]	625	[16]
$MgFe_2O_4$	217	333	486	554	715	[26]

[a] Note the systematic shift of 30–38 rcm^{-1} between the results of this study (as well as other studies given in Table 2), and that of Graves [16]. The synthetic sample used in Grave's study had many defects and, possibly, partial disorder. We attribute the shift to the nature of Graves' sample. This is taken it into the consideration when comparing the Raman frequencies.

[b] Graves [16] assigned this mode to A_{1g}, but later studies [1,7] including our work, undoubtedly show that, at least in the case of magnetite, this mode is of the T_{2g} symmetry.

410–420 and 1322 rcm^{-1}. These belong to the characteristic signature of hematite [22–24]. The peak at 160 rcm^{-1} may be a possible candidate for the lowest frequency phonon mode T_{2g}, as suggested by Degiorgi after considering results from the inelastic neutron scattering [9]. Low frequency limit of our experimental set-up prevented us from probing the range below 170 rcm^{-1} but we do believe that the lowest T_{2g} mode is the one we report at 193 rcm^{-1} (Fig. 2) and not the 160 rcm^{-1} mode. In his Raman study, Hart et al. carried out careful search of the region 120–200 rcm^{-1} but did not detect this phonon [8]. The presence of some phonons is sample specific. Nonstoichiometry, presence of vacancies, interstitial cations, and defects in general, may result in an activation of new phonon modes not predicted by group theory. Further arguments come from our polarized experiments presented below. These show, that modes at 193 and 538 rcm^{-1} are of the T_{2g} symmetry, while modes at 306 and 668 rcm^{-1} belong to the E_g and A_{1g} species. The third predicted T_{2g} mode is not observed in our study, but based on the results of Raman studies of other ferrites (Table 3) this mode is expected between 450 and 500 rcm^{-1}. Vibrational mode analysis shows that regardless of the type of ferrite listed in Table 3, the T_{2g} modes originate only from vibrations involving Fe^{3+} and O^{2-}, while bivalent cations are not directly involved. This explains the similarity of Raman frequencies of listed ferrites and strongly suggests that the third T_{2g} mode occurs around 450–490 rcm^{-1} as observed in a study by Graves [16].

The weak peaks at 462 and 472 rcm^{-1} reported by Degiorgi et al. [9] and by Hart et al. [8] at 130 and 300 K, respectively, were identified as an optical magnon excitation following the results from neutron studies. Indeed, group theory predicts one optically active magnon [8]. We note that the intensity of scattering from magnons should be strongly temperature-dependent what does not appear to be the case when comparing the relative intensities in these studies. In both of them, the spectra were taken in the depolarized configuration and positions of these peaks coincide with the expected T_{2g} mode. More studies conducted at low temperatures and/or studies in magnetic field studies are needed in order to clarify this point.

3.1. Polarized Raman study of magnetite

Polarized Raman study on oriented single crystals represents a powerful tool for deducing the symmetry of vibrational modes. The primitive unit cell of magnetite (Fig. 1) contains one $Fe_4^{2.5+}$ unit where iron atoms are coordinated octahedrally (D_{3d}), and two $Fe^{3+}O_4^{2-}$ units with the tetrahedral coordination (T_d). Group-theoretical and lattice-vibration analyses based on the quasi-molecular description of the spinel structure have led to the following description of normal mode motions of the FeO_4 tetrahedron [7]: A_{1g}—symmetric stretch of oxygen atoms along Fe–O bonds, E_g and $T_{2g}(3)$—symmetric and asymmetric bends of oxygen with respect to Fe, respectively, $T_{2g}(2)$—asymmetric stretch of Fe and O, $T_{2g}(1)$—translatory movement of the whole FeO_4. There are zero, or close-to-zero displacements of Fe atoms in modes A_{1g}, E_g, and $T_{2g}(3)$.

The quasi-molecular model has proved to be a very useful concept for a normal mode analysis particularly in complex structures. It relies on the identification of isolated vibrational units of known symmetry, resulting from the existence of bonds with dissimilar strengths (e.g., covalent subunits bonded by ionic, hydrogen, or van der Waals forces). The class of spinels embody a large number of dominantly ionic compounds where the degree of covalency in tetrahedral and octahedral units varies significantly. Suitability of the molecular model may be judged by comparing the bulk moduli of these units determined in high-pressure studies. For example, the large difference between tetrahedral (120 GPa) and octahedral (260 GPa) bulk moduli in $MgAl_2O_4$ [27] suggests good approximation for the normal mode analysis by the quasi-molecular model [28]. On the other hand, compressional studies on magnetite [3,27] show that, in this compound, the bulk moduli are equal (200 GPa). Moreover, the recently discovered itinerancy of octahedral electrons [6] implies a certain degree of an omnidirectional metallic bond. The unusually large line widths (30–40 rcm^{-1}) of Raman bands observed in this work and in other studies have been explained by the strong electron–phonon coupling [4]. These facts may raise questions about the applicability of the molecular model to magnetite. Detailed lattice dynamic studies are required in order to find out how truly the normal mode atomic motions given above represent reality.

Our polarized measurements were conducted on the (100) face of the single crystal of natural magnetite. First, the spectra were taken from the crystal in orientation with coinciding axes of the crystallographic (x, y, z) and laboratory (x', y', z') frames of reference: $x' = x = (100)$, $y' = y = (010)$, $z' = z = (001)$. The corresponding polarizability tensors for the O_h cubic symmetry are as follows:

$$A_{1g}: a\begin{bmatrix}1&0&0\\0&1&0\\0&0&1\end{bmatrix},$$

$$E_g: b\begin{bmatrix}1&0&0\\0&1&0\\0&0&-2\end{bmatrix}, \quad b\sqrt{3}\begin{bmatrix}1&0&0\\0&-1&0\\0&0&0\end{bmatrix},$$

$$T_{2g}: c\begin{bmatrix}0&1&0\\1&0&0\\0&0&0\end{bmatrix}, \quad c\begin{bmatrix}0&0&1\\0&0&0\\1&0&0\end{bmatrix}, \quad c\begin{bmatrix}0&0&0\\0&0&1\\0&1&0\end{bmatrix}.$$

Analysis of the tensor components shows that only the A_{1g} and E_g modes can be observed when the incident and scattered beams are polarized in a parallel way. Therefore, the two peaks at 668 and 306 rcm^{-1} in the spectrum $X(YY)\bar{X}$ (Fig. 3b) are identified as the A_{1g} and E_g modes, although the complete one-to-one assignment requires further experiment. To describe the particular experimental configuration, we use the convention of Damen, Porto, and Tell [29]. It follows that $X(YY)\bar{X}$ represents the back-scattering geometry with X-axis coinciding with the optical axis of the system. Perpendicular polarizations of the incident and scattered light brings the modes about whose tensors contain the components out of the main diagonal. These are the T_{2g} modes. Hence, the two Raman bands at 193 and 536 rcm^{-1} observed in the spectrum $X(YZ)\bar{X}$ (Fig. 3a) must be of the T_{2g} character.

It is obvious that the conclusions regarding the number of expected peaks for a particular choice of polarization strongly depends on the orientation of the single crystal. Change in the relationship between the crystallographic and laboratory frames of reference translates into the new transformed polarization tensors. The analysis of transformations shows that the A_{1g} mode is the only one that remains extinct in a depolarized experiment regardless of the crystal orientation. This makes its recognition straightforward. On the other hand, the intensities of the other modes will vary depending on the crystal orientation. If the orientational dependence is known it allows identification of these modes. We calculated components of the new polarization tensors P' after rotating the crystal by 45° around the x-axis from the initial position. $P' = SPS^{-1}$, where P stands for the untransformed A_{1g}, E_g, and T_{2g} tensors, and S represents transformation matrix for the operation of rotation. The relative intensities of modes for polarized and depolarized measurements were then derived by summing the squares of the corresponding elements of the tensors of each symmetry class. The results given in Table 4 show, that the experimental configuration $X'(Y'Z')\bar{X}'$ reveals the identity of the E_g mode, which becomes the only one having a non-zero component. Thus, the spectrum $X'(Y'Z')\bar{X}'$ in Fig. 3d shows that the band at 306 rcm^{-1} has to be assigned to the E_g mode and, consequently, the second band at 668 rcm^{-1} in the $X(YY)\bar{X}$ experiment belongs to the A_{1g}. Fig. 3c shows the spectrum obtained after switching to configuration with parallel polarizations $X'(Y'Y')\bar{X}'$. A dramatic change in the relative peak intensities is apparent. The close agreement between the predicted and observed changes (Table 4) further confirms the aforementioned assignments.

Table 4
Calculated and observed relative polarizability intensities for single crystal of magnetite when angle between z-axis of crystal and laser's plane of polarization is set to 45° ($X' = X$)

Mode symmetry	Intensities	Polarization of the incident and scattered beam					
		$(Z'Z')$	$(X'X')$	$(Y'Y')$ Fig. 3c	$(X'Y')$	$(Y'Z')$ Fig. 3d	$(X'Z')$
E_g	Calculated	1	4	1	0	3	0
	Observed			1		2.6	
T_{2g}	Calculated	1	0	1	1	0	1
	Observed			1		0.08	
A_{1g}	Calculated	1	1	1	0	0	0
	Observed			1		0	

Table 5 summarizes the symmetry assignments. The sequencing (1,2,3) of the three T_{2g} modes implies specific atomic motions according to the description above. It has been taken from analysis conducted by Verble [7] and relies partially on the close correspondence between the associated Raman and infrared modes. It is also supported by spectroscopic results from other spinels. Comparison with the previously published assignments in Table 5 shows that the mode analysis of this study provides new interpretation of the Raman spectrum of magnetite. In the following sections we comment on the possible origins of the differences.

The modes at 318 and 308 rcm^{-1} observed by Degiorgi et al. [9] and Gasparov et al. [1], respectively, correspond to the mode at 306 rcm^{-1} in our study. The origin of the differences in the reported frequencies can most likely be traced to the low temperature effect in the study by Degiorgi et al. (spectrum taken at 130 K) and to the calibration/sample effect in the study by Gasparov et al. Based on the presence of these bands in the depolarized spectra, these authors assign the T_{2g} symmetry to this mode. However, as noted above, in the depolarized Raman spectrum, the E_g mode will be

Table 5
Summary of the symmetry assignments of Raman modes of magnetite

Raman shift (rcm^{-1})[a]	Mode symmetry					
	This study	Gasparov [1]	Degiorgi [9][b]	Graves [16]	Verble [7][c]	Hart [8][c]
668	A_{1g}	A_{1g}	A_{1g}	A_{1g}	A_{1g}	A_{1g}
538	$T_{2g}(2)$	T_{2g}	E_g or T_{2g}	A_{1g}	$T_{2g}(2)$	T_{2g}
450–490	$T_{2g}(3)$[d]		Magnon	T_{2g}		Magnon
306	E_g	T_{2g}	T_{2g}	E_g	$T_{2g}(3)$	E_g
193	$T_{2g}(1)$	T_{2g}		T_{2g}		

[a] The listed Raman shifts are according to this study. Results from other studies differ typically by several wave numbers and are fully listed in Table 2.
[b] Weak peak at 160 rcm^{-1} assigned to the $T_{2g}(1)$ mode. See the text for the discussion.
[c] The complete assignments in these studies include also lines at 420 and 298 rcm^{-1}, which were identified as two T_{2g} modes in [8], and as the E_g and $T_{2g}(1)$ modes, respectively in [7]. These lines clearly indicate the presence of hematite thus they probably originate from a minor oxidation of magnetite.
[d] Not observed but inferred from spectra of other ferrites. See the text and Table 3.

present along with the T_{2g} modes, unless a single crystal is in a specific orientation. The orientation of the crystal in the two studies is not stated. Our polarized measurements with the oriented crystal clearly show E_g symmetry for this mode.

Table 2 shows that some studies report two additional Raman bands at around 300 and 410–420 rcm^{-1}. We note that these lines belong to the characteristic features of spectrum of hematite representing the $E_g(3)$ and $E_g(4)$ modes, respectively [22]. It is well known [30] that bivalent iron makes magnetite easily prone to oxidation. Temperature plays a dominant role in this process. We have conducted a thorough study on the effect of laser power on the Raman spectrum of magnetite. The full details will be presented elsewhere, here we discuss them only briefly to the extent, which helps us to resolve the reported discrepancies in the Raman spectra of magnetite. The results show that in a micro-Raman experiment, when an excitation laser is focused to a spot with diameter of only several μm, the use of laser power even as low as several tens mW can result in a temperature increase by several hundreds of degrees. For a powdered magnetite, laser power well below 25 mW caused a rapid oxidation. Series of Raman spectra collected at a stepwise increase of the laser power gradually started to show the hematite bands. The first recognizable features of hematite appeared at about 300 and 410 rcm^{-1}. Upon further increase of laser power their intensity grew dramatically and dominated the spectra. Fig. 4 shows the result of Raman experiment on magnetite conducted in air and using 65 mW of laser power at 514.5 nm. The spectrum essentially corresponds to that of hematite, except for the presence of a residual peak of magnetite at 668 rcm^{-1}. We also found that the Raman scattering power of hematite is much larger that the scattering power of magnetite. As a result, even a very small amount of hematite causes the presence of spurious peaks in the Raman spectrum of magnetite. It is not unlikely that the peaks at 300 and 410–420 rcm^{-1} reported in some studies on magnetite were due to a minor amount of oxidation in the course of the Raman experiment.

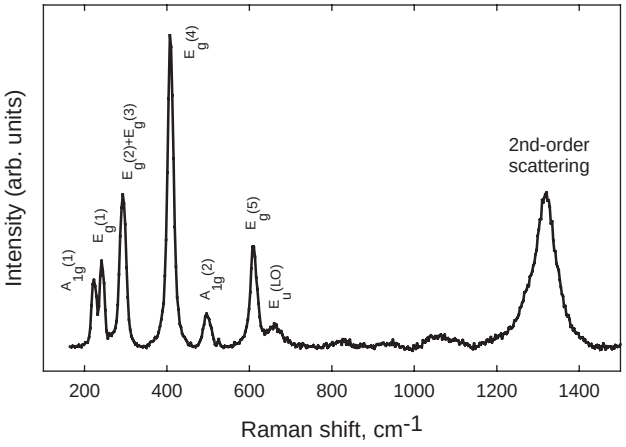

Fig. 4. Raman spectrum collected from the sample of magnetite subjected to 65 mW of laser power. The pattern is identified as a spectrum of hematite and the assignment follows study [22].

4. Summary and conclusions

A detailed Raman study on natural magnetite has been carried out. Raman spectra show four out of the five predicted Raman bands located at 668, 538, 306, and 193 rcm^{-1}. The location of the fifth, unobserved phonon mode, is inferred from spectra of other ferrites at 450–490 rcm^{-1}. Polarized experiments on the oriented single crystal provide a new interpretation of the Raman spectrum with the following assignment for symmetries of the observed modes: A_{1g} for 668 rcm^{-1}, E_g for 306 rcm^{-1}, and T_{2g} for 538 rcm^{-1}, 193 rcm^{-1}, and 450–490 rcm^{-1}.

Group theory predicts number and symmetries of Raman and infrared bands but the intensities of bands have to be derived from lattice dynamics calculations. The results of this and other studies suggest that the amplitude of scattering of the unobserved fifth phonon mode is very low. Further Raman studies conducted well below ambient temperatures, and using ultra-sensitive CCD detectors may result in the experimental detection of this elusive phonon. Likewise, the application of an external magnetic field may greatly aid in the reliable identification of the optically active magnon in Raman studies. Raman spectra may vary between different samples of magnetite. Aside from changes resulting from possible defect structures and presence of vacancies and interstitial cations, there exist a large number of cation ordering schemes between the octahedral and tetrahedral sites [31,32]. Group-theory analysis predicts dramatically increased number of optically active modes.

Ideally, precise Raman experiments on magnetite should be conducted under strictly controlled conditions. Oxygen fugacity should be controlled and reported. Some differences in the reported Raman frequencies can most likely be attributed to the temperature effects. Increased temperature of a laser heated spot results in a softening of phonon frequency. Considering a typical thermal shift of $0.02\,cm^{-1}/K$, the observed difference of 1–2 wavenumbers in reported frequencies between various studies may be due to the fact that the temperature effect has not been taken into account.

Acknowledgments

We thank Prof. Hans Annersten for providing the sample of natural magnetite. The Swedish Research Council (Vetenskapsrådet) is gratefully acknowledged for the financial support.

References

[1] L.V. Gasparov, D.B. Tanner, D.B. Romero, H. Berger, G. Margaritondo, L. Forro, Phys. Rev. B. 62 (2000) 7939–7944.
[2] Y. Fei, D.J. Frost, H. Mao, C.T. Prewitt, D. Häusermann, Am. Mineral. 84 (1999) 203–206.
[3] C. Haavik, S. Stolen, H. Fjellvåg, M. Hanfland, D. Häusermann, Am. Mineral. 85 (2000) 514–523.
[4] R. Gupta, A.K. Sood, P. Metcalf, J.M. Honig, Phys. Rev. B 65 (2002) 104430-1-8.
[5] J. García, G. Subías, M.G. Proietti, H. Renevier, Y. Joly, J.L. Hodeau, J. Blasko, M.C. Sánchez, J.F. Bérar, Phys. Rev. Lett. 85 (2000) 578–581.
[6] Yu. S. Dedkov, U. Rüdiger, G. Güntherodt, Phys. Rev. B. 65 (2002) 064417-1-5.
[7] J.L. Verble, Phys. Rev. B. 9 (1974) 5236–5248.
[8] T.R. Hart, S.B. Adams, H. Tempkin, in: M. Balkanski, R. Leite, S. Porto (Eds.), Proceedings of the 3rd International Conference on Light Scattering in Solids, Flammarion, Paris, 1976, pp. 254–258.
[9] L. Degiorgi, I. Blatter-Mörke, P. Wachter, Phys. Rev. B 35 (1987–) 5421–5424.
[10] D.L.A. de Faria, S. Venâncio Silva, M.T. de Oliveira, J. Raman Spectrosc. 28 (1997) 873–878.
[11] J.-M. Li, A.C.H. Huan, Phys. Rev. B 61 (2000) 6876–6878.
[12] T. Ohtsuka, K. Kubo, N. Sato, Corrosion 42 (1986) 476.
[13] D. Thierry, D. Persson, C. Leygraf, N. Boucherit, A. Hugot-Le Goff, Corros. Sci. 32 (1991) 273.
[14] J. Dünnwald, A. Otto, Corros. Sci. 29 (1989) 1167–1176.
[15] N. Boucherit, A. Hugot-Le Goff, S. Joiret, Corros. Sci. 32 (1991) 497.
[16] P.R. Graves, C. Johnston, J.J. Campaniello, Mater. Res. Bull. 23 (1988) 1651–1660.
[17] H. Annersten, T. Ekström, Lithos 4 (1971) 185–204.
[18] M.E. Fleet, Acta Cryst. B 38 (1982) 1718–1723.
[19] W.B. White, B.A. DeAngelis, Spectrochim. Acta 23A (1967) 985–995.
[20] N.W. Grimes, Philos. Mag. 26 (1972) 1217–1226.
[21] N.W. Grimes, P. Thompson, H.F. Kay, Proc. R. Soc. Lond. A 386 (1983) 333–345.
[22] I.R. Beattie, T.R. Gilson, J. Chem. Soc. A 5 (1970) 980–986.
[23] M.J. Massey, U. Baier, R. Merlin, W.H. Weber, Phys. Rev. B. Condens.: Matter 41 (1990) 7822–7827.
[24] S.-H. Shim, T.S. Duffy, Am. Mineral. 87 (2002) 318–326.
[25] D. Bersani, P.P. Lottici, A. Montenero, J. Raman Spectrosc. 30 (1999) 355–360.
[26] Z. Wang, P. Lazor, S.K. Saxena, H.S.C. O'Neill, Mat. Res. Bull. 37 (2002) 1589–1602.
[27] L.W. Finger, R.M. Hazen, A.M. Hofmeister, Phys. Chem. Minerals 13 (1986) 215–220.
[28] A. Chopelas, A.M. Hofmeister, Phys. Chem. Minerals 18 (1991) 279–293.
[29] T.C. Damen, S.P.S. Porto, B. Tell, Phys. Rev. 142 (1966) 570–574.
[30] W. Feitknecht, K.J. Gallagher, Nature 228 (1970) 548–549.
[31] V.G. Keramidas, B.A. Deangelis, W.B. White, J. Solid State Chem. 15 (1975) 233–245.
[32] W.B. White, V.G. Keramidas, Solid state chemistry, Proceedings of 5th Materials Research Symposium, National Bureau of Standards Special Publication 364, Gaithersburg, MD, USA, 1972, pp. 113–126.